α -Lipoic Acid-Plus Ameliorates Endothelial Injury via Inhibiting the Apoptosis Pathway Mediated by Intralysosomal Cathepsins in Vivo and Vitro Endothelial Injury Model

Yang Wang
The First Affiliated Hospital of USTC: Anhui Provincial Hospital
Xiangqian Kong
Shandong Provincial Hospital
Dejun Bao
The First Affiliated Hospital of USTC: Anhui Provincial Hospital
Bin xu
Anhui Medical College
Yongfei Dong
The First Affiliated Hospital of USTC: Anhui Provincial Hospital
Xiangping Wei
The First Affiliated Hospital of USTC: Anhui Provincial Hospital
Chaoshi Niu (ah_neurosurgery@163.com)
The First Affiliated Hospital of USTC, Division of Life Sciences and Medicine, University of Science and Technology of China

Research Article

Keywords: α-Lipoic acid-plus, Human umbilical vein endothelial cells, Intimal injury, CathepsinB/D, Iron overload

Posted Date: February 10th, 2021

DOI: https://doi.org/10.21203/rs.3.rs-180944/v1

Abstract

Purpose

We tried to explore the potential role of the α-Lipoic acid-plus (LAP) in endothelial injury *in vitro* and *vivo* models. Simultaneously, possible endovascular protective mechanisms of LAP were also investigated further.

Methods

In vitro, oxyhemoglobin (OxyHb) stimulating human umbilical vein endothelial cells (HUVECs) simulated intimal injury. *In vivo*, carotid artery angioplasty injury was used to generate a model of rat carotid artery intimal injury (CAII). HUVECs and rats were treated with desferrioxamine (DFO) and LAP.

Results

In experiment 1, we found that the expressions of Cathepsin B/D in endothelial tissue increased and reached peak point in 48 hours post rat CAII. In experiment 2, firstly, the protein levels of Cathepsin B/D, cleaved-caspase-3, Bax, Ferritin, Transferrin Receptor (TfR) markedly increased after CAII and reversed by DFO and LAP treatments. Besides, DFO and LAP treatments also reduced oxidative stress level and endothelial cells (ECs) necrosis of the damaged endometrium. In experiment 3, firstly, the protein levels of Cathepsin B/D, cleaved-caspase-3, Bax, Ferritin and TfR apparently increased post OxyHb stimulation, which were further aggravated by the addition of iron and decreased by DFO and LAP treatments. Moreover, DFO and LAP significantly ameliorated oxidative stress level, HUVECs injury, iron level, mitochondrial damage and were beneficial to maintain lysosomal integrity. Finally, LAP may have exerted more significant endovascular protective effects than DFO.

Conclusions

LAP probably exerted endovascular protective effects via inhibiting the apoptosis pathway mediated by intralysosomal Cathepsins by chelating excessive iron in endothelial lysosomes post intimal injury.

Introduction

Carotid artery stenosis is a recognized risk factor of ischemic stroke, contributing to up to 10%-20% of strokes or transient ischemic attacks [1]. Although precautionary medical treatment have increased, the proportion requiring surgical intervention remains high [2]. Both open operation and interventional surgery can induce different degrees of vascular injury, which triggers a cascade of reaction aimed at maintaining vascular homeostasis. In brief, the repair process of blood vessels comprises injured site reendothelialization, vascular remodeling, and intimal hyperplasia (IH) formation [3, 4]. Excessive IH formation is the primary cause of restenosis and vascular interventions therapy failure [5]. Endothelial cells (ECs) injury is identified as the first step toward postoperative IH formation [6]. The injured site is

tors and the ability of regulation of vascular homeostasis is

further weakened. The damaged area is coated with platelets, fibrinogen, circulating RBCs and macrophages that release thrombotic factors (fibrinogen and Von Willebrand factor) and growth factors (platelet-derived growth factor and transforming growth factor). Among them, the toxic effects of erythrocyte metabolites, especially the release of catalytically redox-active iron, are often neglected by us [7]. Reendothelialization represents an important process in vascular healing depending on migration and proliferation of ECs [8]. Thus, stimulation of ECs proliferation and migration is critical in order to promote endothelial healing and improve vascular function in response to loss of ECs resulting from intimal injury. The occurrence of delayed reendothelialization is one of the important causes of excessive IH due to ECs apoptosis and degeneration.

Iron is an important and necessary element for human growth and development, which is not only used for hemoglobin synthesis but also participated in mitochondrial respiration and DNA replication. However, iron is also a “double-edged sword”, excessive iron intake causes the damage of cells, organs, and even the entire body, which has raised sufficient attention [9]. Iron increased the production of reactive oxygen species (ROS) and calcium influx into mitochondria, which disturbed mitochondrial respiration function and eventually led to loss of mitochondrial membrane potential ($\Delta\Psi m$). A significant increase in apoptotic cells and endothelial microparticles (EMPs) were found under iron intervention [10]. ROS plays an important role in the pathophysiological process of cells and tissues caused by iron overload and have pathological significance in a wide range of cardiovascular and endothelial dysfunctions [11]. Iron overload can cause excessive ROS generation by participating in the Fenton reaction, resulting in mitochondrial membrane depolarization, mitochondrial permeability increase, cytochrome c (cyt c) releasing into the cytoplasm, caspase family activating, and ultimately leading to cells apoptosis. In addition, iron overload and iron-mediated free radical production cause loss of tight junction proteins and degeneration of ECs, then leading to opening of the blood-brain barrier (BBB) after transient forebrain ischemia [12]. The previous literature manifests that iron induces EMPs generation and ECs apoptosis in association with increased oxidative stress. Therefore, iron overload has been regarded as a risk factor for cardiovascular events [13]. In this experiment, we aim to investigate the effects of redox-active iron on ECs status *in vitro* and *vivo* condition and relevant damage mechanisms.

As a radical scavenger, α-lipoic acid (LAP) has been demonstrated to exert neuroprotective effects in rat models of subarachnoid hemorrhage (SAH). According to the previous literatures, we discovered LAP containing a weak base (pKa = 8.0), should be easier to get into lysosomes (PH = 4.6-5.0) via proton trapping approach. In addition, the reduced forms of LAP, namely DHLAP, could supply sulfydryl to interact with iron [14, 15]. The structures of DFO, LAP and DHLAP were shown in Fig. 1. Though LAP could protect cells against oxidant challenges in vivo and alleviate early brain injury after SAH, whether LAP could inhibit endovascular injury induced by balloon compression and the underlying mechanisms were still not investigated deeply. Therefore, the purpose of this study was to evaluate the role of LAP in the reduction of ECs apoptosis via the regulation of oxidative stress, with the goal of identifying novel medication for the treatment of carotid artery intimal injury (CAII).

Methods

Experimental animals

Experiments were approved by the Ethics Committee of the First Affiliated Hospital of University of Science and Technology of China and were performed in accordance with the guidelines of the National Institutes of Health on the care and use of animals. Adult male Sprague-Dawley (SD) rats weighing between 270 and 300 g were used in this experiment and purchased from Zhaoyan New Drug Research Center (Suzhou, China) Co., LTD. The rats were housed in temperature- and humidity-controlled animal quarters with a 12-h light/dark cycle. Animal body temperature was maintained at 37˚C.

Experimental design and intervention

Experiment 1 was designed for confirming involvement of the cathepsin B/D in endothelium following CA intimal injury (CAII). In experiment 1, 54 rats were stochasticly assigned to 9 groups (n = 6): Sham, 6-, 12-, 24-, 48-, 72-hour, 1-week, 2-week and 4-week CAII groups. The CAs collected from Sham and CAII rats at different time points for western blot, immunofluorescence (IF) assay. The whole experimental flow is shown in Fig. 2a. Experiment 2 was designed for exploring the mechanisms of LAP alleviating endothelial injury induced by CAII. In experiment 2, 90 male SD rats were randomly divided into 7 groups of 18 rats each: Sham group, CAII, CAII + vehicle group, CAII + DFO (25mg/kg), CAII + LAP (100 mg/kg) group, CAII + LAP (150 mg/kg) group, CAII + LAP (200 mg/kg) group. LAP was synthesized by LA (branch company of Agilent Technologies, Beijing, China) and mixed with 0.5 % methylcellulose (Sinopharm Chemical Reagent Co., Ltd, Shanghai, China) before oral administration. DFO was administered through intraperitoneal injection and LAP was administered through an orogastric tube at 4 h after the induction of CAII and continued for 48 h once a day. The dose of DFO and LAP administered was based on previous study [15, 16]. 6 rats CAs in every group were cut into slices and used for IF staining and Fluoro-Jade B (FJB) staining. The remaining 6 rats in every group were executed, perfused and brain tissue samples collected for western blot assay and oxidative stress evaluation. The experimental flow is displayed in Fig. 2b. Experiment 3 was designed for exploring the roles and mechanisms of LAP alleviating Human umbilical vein endothelial cells (HUVECs) injury induced by OxyHb in vitro. In experiment 3, logarithmically growing HUVECs were divided into 7 groups: Control, OxyHb, OxyHb + Iron, OxyHb + DFO, OxyHb + LAP-L, OxyHb + LAP-M, OxyHb + LAP-H groups. HUVECs were exposed to OxyHb (10μM) and DFO (1 mM) or LAP (0.2 μM, 0.3 μM and 0.4 μM) were treated for 24 h prior to conducting any subsequent assays [14]. After the treatments, firstly, the living cell were collected for cell viability assays, Lactate dehydrogenase assay (LDH), AO staining, Live-dead cells staining, Lyso-Tracker Red, Measurement of mitochondrial membrane potential (MMP) and oxidative stress evaluation. Secondly, HUVECs was fixed with paraformaldehyde for IF staining. Total protein of HUVECs was collected for western blot assay. Specific experimental procedures were displayed in Fig. 2C.

Rat carotid artery balloon injury model

A right CAII was established based on an approach described in our previous literature [17]. Specific stereotactic head frame was designed and manufactured by the experimental group members. In addition, a catheter and balloon were purchased from Medtronic Inc. and manufactured by the group members of this experiment. A T-branch pipe and 1-ml syringe were used to modulate the size and pressure of the balloon. Briefly, the catheter was inserted through the external CA and slipped into the common CA, where it was inflated to ~2 atm and the inner surface of the common CA was rubbed back and forth three times. The catheter was then removed and the impaired external CA was sutured tightly using a 12-0 proline under the operating microscope (M651; Leica Microsystems). The 2-cm common CA injured region was cut for analysis in this experiment.

Cell culture and treatment

HUVECs were obtained and cultured as described previously [18]. To evaluate the effect of LAP *in vitro*, the HUVECs were exposed to LAP at a gradient concentration for 24 h prior to conducting any subsequent assays.

Western blot analysis

Western blot analysis was performed as described previously [19]. The CAs were added into cell lysis buffer and grounded. The lysates were centrifuged at 12,000 g for 10 min at 4°C twice, subsequently, the supernatant was extracted and the protein concentration was measured by Enhanced BCA protein assay kit. Protein samples (12 μg/lane) were loaded, separated, electrophoreted and transmembraneed. The nitrocellulose filter membranes were blocked with 5% bovine serum albumin (BSA; BioSharp, Hefei, AH, China) for 1 h at room temperature and then incubated overnight at 4˚C with primary antibodies of Cathepsin B (1:2000, ab214428, abcam), Cathepsin D (1:1000, #2284s, Cell Signaling Technology), Cleaved Caspase-3 (1:1000, ab2302, abcam), Bax (1:1000, ab182733, abcam), Ferritin (1:1000, ab75973, abcam) and Transferrin Receptor (TfR) (1:1000, ab269513, abcam). Next, the membranes were washed three times and incubated with the anti-mouse IgG, horseradish peroxidase conjugated-linked-secondary antibody and anti-rabbit IgG, horseradish peroxidase conjugated-linked-secondary antibody (1:3000, 7076S and 7074s, Cell Signaling Technology, Boston, MA, USA) for 2 h at room temperature. Finally, the display of protein bands was detected with a luminescent image analyzer (Clinx ChemiScope5300, Clinx Science Instruments, Shanghai, China). The protein levels were analyzed with ImageJ software (National Institutes of Health, Bethesda, MD, USA) and normalized to the relative density of the sham or control group.

IF microscopy

The injured CA was excised, fixed, embedded in paraffin and cut into 4-μm sections and examined by IF staining. Homoplastically, the disposed HUVECs were fixed by 4% paraformaldehyde. As previously described [20], The sections and HUVECs were incubated with primary antibodies to Cathepsin B (1:100, ab214428, abcam), Cathepsin D (1:200, #2284s, Cell Signaling Technology), Ferritin (1:50, ab75973, t 4°C overnight. Then, it was incubated with the Donkey anti-

Rabbit IgG (H+L) Highly Cross-Adsorbed Secondary Antibody, Alexa Fluor 488 (1:300, A32790, Invitrogen) and Alexa Fluor 555 (1:300, A32794, Invitrogen) and Goat anti-Mouse IgG (H+L) Cross-Adsorbed Secondary Antibody, Alexa Fluor 488 (1:300, A-11001, Invitrogen) and Alexa Fluor 555 (1:300, A-21424, Invitrogen) at 37°C for 1 hour after washed 3 times on the following day. Next, the sections were added into 4,6-diamino-2-phenylindole (SouthernBiotech, Birmingham, AL, USA) for coverslipping. In the end, the sections were observed under a fluorescence microscopeOLYMPUS BX50/BX-FLA/DP70; Olympus Co., Japan, and ImageJ software was used for quantizing the fluorescence intensity.

Prussian blue reaction

Intracellular and intralysosomal iron level of HUVECs was estimated approximately by Prussian blue reaction of living HUVECs according to the manufacturer's programs (G1422, Solarbio, Beijing, China). The results were observed under a light microscope (×100) in accordance with the approach described in a previous literature [21].

Oxidative stress indicator assay

The concentrations of ROS and MDA and activitives of SOD and GSH-Px in the impaired CAs and HUVECs were measured by detection kits (E004-1-1, A003-1-2, A001-3-2, A005-1-2, Nanjing Jiancheng Bioengineering Institute, Jiangsu, China), as per the manufacturer's instructions, and as previously described [22].

FJB staining

FJB is a hypersensitive and specific fluorescent dye that can be used to indicate ECs degradation and the operation process was based on the previous literature [23]. Briefly, the CA sections were immersed in 0.06% $KMnO_4$ solution in dark environment at room temperature for 15 minutes after being dewaxed. Next, the sections were added and incubated with FJB working solution (AG310, Sigma-Aldrich, St. Louis, Missouri, USA) (adding 0.1% acetic acid solvent) for 1 hour after being washed. Then, the sections were air-dried at fuming cupboard. Finally, the stained sections were sealed with neutral balsam mounting medium and observed in fluorescence microscope and take photos in parallel to count FJB-positive cells.

Cell viability assays

After indicated treatments, the HUVECs were fixed with 50% trichloroacetic acid and stained with a sulforhodamine B (SRB) solution (230162, Sigma-Aldrich, St. Louis, Missouri, USA) as described previously [24]. Next, SRB was measured from the absorbance at 565 nm wave length using a BioRad microplate reader. The assay was performed in triplicate and repeated at least three times independently.

Lactate dehydrogenase (LDH) assay

Based on the manufacturer's protocol of LDH assay kit (C0016; Beyotime Institute of Biotechnology, Shanghai, China), the LDH assay was performed to evaluate apoptosis and necrosis of cultured HUVECs

[25].

Live-dead cells staining in vitro

HUVECs apoptosis was examined by live-dead cells staining at 48 hours after OxyHb and iron interventions. We used calcein-AM/propidium iodide double-stain kit (Thermo Fisher Scientific, Shanghai, China) to detect cultured HUVECs apoptosis according to the manual [26]. Primarily, culture medium was removed and living HUVECs were washed for 3 times. Next, the pre-configured working reagent mixed with calcein-AM and propidium iodide was added into the HUVECs and incubated for half 1 hour at room temperature. Finally, the apoptosis rate was analyzed and counted under a fluorescence microscope.

AO staining

HUVECs at logarithmic growth stage were planted into 24-well plates. The cells continued to be cultivated for 24 h. Then, the original culture medium was removed from each hole, and 1 ml culture medium containing corresponding concentrations of OxyHb, DFO and LAP was added to each hole respectively. Next, the original culture medium in each hole was removed and washed with PBS post continuous culture for 24h. AO dye solution (A7847, Sigma-Aldrich, Missouri, USA) was added and reacted at room temperature for 1 min. Finally, the cells were observed, photographed and recorded under a fluorescence microscope after the PBS buffer was removed and the cells were washed [27].

Lyso-Tracker Red

1μl Lyso-Tracker Red solution was added to 20ml cell culture medium and mixed to form Lyso-Tracker Red working solution. Then, cell culture medium was removed, and the lyso-Tracker Red working solution preincubated at 37℃ was added. Next, The cells continued to be incubated for 30-120 minutes at 37℃. Finally, Lyso-Tracker Red working solution was removed and new cell culture solution was added again. The lysosomes in the cytoplasm were stained with bright and intense fluorescence under fluorescence microscopy.

Measurement of mitochondrial membrane potential (MMP)

The MMP was detected with a JC-1 kit (Beyotime, Shanghai, China) according to the instruction book [26]. HUVECs in culture media within 12-well plates were washed with PBS and treated with JC-1 work solution in the dark room for 20 minutes. At last, the cultured cells were analyzed under a fluorescent microscope.

Statistical analysis

GraphPad Prism 7.0 software (San Diego, California, USA) was used for data processing and analyzing. The data was shown as the mean ± SEM (standard error of mean). One-way or two-way Analysis of Variance (ANOVA) was used for multiple comparisons, and Bonferroni's or Tukey's *post hoc* test was used

for comparison between two pairs in multiple groups. $P < 0.05$ was considered as significantly statistical standard.

Results

Cathepsin B/D is activated following CAII

To detect the changes of Cathepsin B/D expressions after CAII, western blot and IF were performed. Western blot results manifested that the expressions of Cathepsin B/D obviously increased after CAII, attained the highest peak at 48 hours, and then gradually recovered within 4 week ($P < 0.05$ or $P < 0.01$ or $P < 0.001$; Fig. 3a-d). Simultaneously, IF also showed that the immunopositivities of Cathepsin B/D increased at each time points after SAH compared with Sham group ($P < 0.01$; Fig. 3e-h). These above results indicated that the Cathepsin B/D may participate in the pathological process during CAII, and is apparently activated following CAII. Further, 48 hours after CAII might be the most appropriate time point for intervention in experiment 2. Therefore, 48 hours was regarded as an optimal intervention point in further study.

DFO and different gradient concentration LAP alleviated Cathepsin B/D, cleaved-caspase-3 and Bax expression levels after experimental CAII

Western blot was applied to assess target protein expression in the CAs tissue after treatments with DFO and different concentrations of LAP (Fig. 4a-f). The results displayed that the expressions of Cathepsin B/D, cleaved-caspase-3 and Bax in CAII and CAII + Vehicle groups appeared a distinct rise than Sham group ($P < 0.05$ or $P < 0.001$). In contrast, the expressions of Cathepsin B/D, cleaved-caspase-3 and Bax in CAII + DFO, and CAII + LAP groups were decreased in comparison with CAII + Vehicle group respectively ($P < 0.01$ or $P < 0.001$). It's worth noting that high dose of LAP further attenuated Cathepsin B/D, cleaved-caspase-3 and Bax expressions compared with DFO group respectively ($P < 0.05$ or $P < 0.01$). Moreover, immunofluorescent staining also showed that the similar trends in Cathepsin B/D, cleaved-caspase-3 and Bax after SAH (Fig. 4g-j)

DFO and different gradient concentration LAP alleviated Cathepsin B/D, cleaved-caspase-3 and Bax expression levels post HUVECs injury

Western blot was applied to assess target protein expression in the HUVECs **a**fter treatments with DFO and different concentrations of LAP (Fig. 5a-f). The results displayed that the expressions of Cathepsin B/D, cleaved-caspase-3 and Bax in OxyHb group appeared a distinct rise than Control group ($P < 0.05$ or $P < 0.01$ or $P < 0.001$). In contrast, Iron treatment further increased the levels of Cathepsin B/D, cleaved-caspase-3, Bax and LAP decreased the levels of Cathepsin B/D, cleaved-caspase-3 and Bax respectively ($P < 0.05$ or $P < 0.01$ or $P < 0.001$). It's worth noting that high dose of LAP further attenuated Cathepsin B/D, cleaved-caspase-3, Bax expressions compared with DFO group respectively ($P < 0.05$ or $P < 0.01$ or $P < 0.001$). Moreover, immunofluorescent staining also showed that the similar trends in Cathepsin B/D,

ury by OxyHb stimulation.

DFO and different gradient concentration LAP alleviated oxidative stress level under endothelium and HUVECs injury condition

The assay of oxidative stress indicators was shown in CAs tissue (Fig. 6a–d) and HUVECs (Fig. 6e–h). In the CAII + Vehicle group, the average levels of ROS and MDA in the CAs samples showed a marked increase, as compared with the Sham group ($P < 0.05$ or $P < 0.01$), while DFO and LAP administration abolished the elevation in the CAs tissue ($P < 0.05$ or $P < 0.01$). Conversely, CAII caused a significant depletion of SOD and GSH-Px activitives in CAs ($P < 0.05$ or $P < 0.001$), while DFO + LAP could significantly suppress the reduction of SOD and GSH-Px activities ($P < 0.05$ or $P < 0.01$or $P < 0.001$). In the OxyHb + Vehicle group, the average levels of ROS and MDA in the HUVECs showed a marked increase, as compared with the Control group ($P < 0.05$ or $P < 0.01$). Moreover, Iron treatment further increased average levels of ROS and MDA under OxyHb treatment condition ($P < 0.05$ or $P < 0.01$). while LAP administration abolished the elevation in the HUVECs ($P < 0.05$ or $P < 0.01$). Conversely, OxyHb caused a significant depletion of SOD and GSH-Px activities in HUVECs ($P < 0.05$ or $P < 0.001$), while LAP could significantly suppress the reduction of SOD and GSH-Px activities ($P < 0.05$ or $P < 0.01$). On the whole, LAP was a more potent antioxidant than DFO because the comparative results revealed high dose of LAP reduced the indexes about oxidative stress more strongly than DFO ($P < 0.05$ or $P < 0.01$).

LAP could rescue damaged HUVECs in vitro

The results of live-dead cellular staining was used to evaluate the survival rate of HUVECs (Fig. 7a, b). The staining for live (green) and dead (red) cells also showed that the survival rate of HUVECs in OxyHb group was lower than Control group ($P < 0.001$). However, Iron-treated group had a lower survival rate than did those in the OxyHb group, and the HUVECs of the OxyHb + LAP-treated group had higher survival rate than did those in the OxyHb group ($P < 0.01$ or $P < 0.001$). Middle dose and high dose LAP-treated group exerted more significantly protective effect than DFO ($P < 0.05$ or $P < 0.01$). The SRB assay was used to measure the viability of cells (Fig. 7c). The result showed that OxyHb significantly decreased the viability of HUVECs ($P < 0.001$). In contrast, Iron treatment further decreased the viability of HUVECs post OxyHb treatment ($P < 0.01$). Compared with the OxyHb group, the cell viability in the OxyHb + LAP-treated group markedly increased ($P < 0.001$). It is certain that high dose LAP further increased the cell viability of HUVECs than DFO ($P < 0.05$). Consistently, the LDH assay was used to measure the necrosis of HUVECs (Fig. 7d). OxyHb apparently increased the activity of LDH compared with Control group ($P < 0.001$) and Iron treatment further decreased the activity of LDH post OxyHb treatment ($P < 0.001$). Compared with the OxyHb group, the activity of LDH in the OxyHb + LAP-treated group markedly decreased ($P < 0.05$ or $P < 0.01$ or $P < 0.001$). It is certain that high dose LAP further decreased the activity of LDH than DFO ($P < 0.01$). In addition, FJB staining showed no FJB-positive cells in the Sham group (Fig. 7e), whereas the number of FJB-positive cells was significantly higher in the CAII group. Compared with the CAII + Vehicle group, the amount of FJB-positive cells was significantly attenuated by DFO and LAP. Together, these results suggested that the LAP had vascular protective effects than DFO.

LAP promotes mitochondrial transport and distribution in damaged HUVECs in vitro

Immunofluorescent staining showed that the similar trends in mitochondria marker ATPB post HUVECs injury by OxyHb stimulation (Fig. 8a). The immunofluorescent intensity of ATPB was evaluate the mitochondrial survival. The result showed that OxyHb significantly decreased immunofluorescent intensity of ATPB ($P < 0.001$). In contrast, Iron treatment further decreased immunofluorescent intensity of ATPB post OxyHb treatment ($P < 0.05$). Compared with the OxyHb group, immunofluorescent intensity of ATPB in the OxyHb + LAP-treated group markedly increased ATPB expression ($P < 0.05$ or $P < 0.001$). It is certain that high dose LAP further increased ATPB expression of HUVECs than DFO ($P < 0.05$). To study the effect on mitochondrial damage by LAP, we stained HUVECs *in vitro* with the cationic lipophilic dye, JC-1. In healthy mitochondria of HUVECs, JC-1 shown red fluorescence, while in damaged mitochondria of HUVECs, JC-1 transforms into green fluorescence (Fig. 8b, d). The results showed the percentage of green-fluorescent-positive signal in OxyHb group was brighter than Control group ($P < 0.001$), while Iron treatment further increased the percentage of green-fluorescent-positive signal ($P < 0.05$). In contrast, compared with that in the OxyHb + DFO- and OxyHb + LAP-treated group, the percentage of green-fluorescent-positive signal was lower than OxyHb + group ($P < 0.05$ or $P < 0.001$). It is undeniable that middle and high dose of LAP decreased the percentage of green-fluorescent-positive signal than DFO ($P < 0.01$ or $P < 0.001$).

DFO and different gradient concentration LAP alleviated Ferritin and TfR expression levels and Iron deposition post endothelium and HUVECs injury

Western blot was applied to assess Ferritin and TfR expression in the HUVECs after treatments with DFO and different concentrations of LAP (Fig. 9a-f). The results displayed that the expressions of Ferritin and TfR in CAII group and OxyHb group appeared a distinct rise than control group ($P < 0.05$ or $P < 0.001$). In contrast, Iron treatment further increased the levels of Ferritin and TfR of HUVECs. However, DFO and LAP decreased the levels of Ferritin and TfR in endothelium and HUVECs respectively ($P < 0.05$ or $P < 0.01$ or $P < 0.001$). It's worth noting that middle and high dose of LAP further attenuated Ferritin and TfR expressions compared with DFO respectively ($P < 0.05$ or $P < 0.01$ or $P < 0.001$). Moreover, immunofluorescent staining also showed that the similar trends of Ferritin and TfR expressions post HUVECs injury (Fig. 9g-j). Prussian blue reaction were performed iron content in HUVECs (Fig. 9k). In the Control group, little iron deposition in the HUVECs could be clearly observed, while in OxyHb group, we observed more significant iron deposition in the HUVECs. Compared to OxyHb group, iron deposition in HUVECs was markedly increased by Iron addition and reduced by DFO and oral administration of LAP. In addition, high dose of LAP seems an added extra effect on inhibiting iron deposition than DFO and low dose LAP.

LAP treatments alleviated the LMP and protected the lysosomes from rupture

To detect the state and quantity of lysosomes in HUVECs, immunofluorescence stainings was performed with LAMP-1 attached to different dosage groups (Fig. 10a). A marked decrease of LAMP-1 expression was observed in OxyHb group, Iron treatment further reduced LAMP-1 expression. DFO and different doses of LAP remarkablely inhibited lysosome rupture in accordance with the alteration of LAMP-1

fluorescent intensity of in HUVECs. But high dose of LAP treatment seemingly had a more effect on stabilizing lysosomal membrane than other doses of LAP and DFO. As a preliminary indicator of lysosomal state, the acidic compartments in HUVECs were observed by AO staining and Lyso-Tracker Red staining. As shown in Fig. 10b, c, there was a normal amount of accumulation of acidic compartments in HUVECs in the Control group. The accumulation of acidic compartments in HUVECs was significantly decreased compared with that in the Control group post OxyHb and Iron treatment. However, the accumulation of acidic compartments in HUVECs was significantly increased post DFO and LAP treatments.

Discussion

Our results in experiment 1 proved that the apoptosis pathway mediated by intralysosomal Cathepsins was activated and the expressions of Cathepsin B/D were elevated in damaged blood vessel tissue, with the most noticeable activation time point being 48 hours after intimal injury. In experiment 2, we found that DFO and LAP treatments both inhibited the apoptosis pathway mediated by intralysosomal Cathepsins by reducing the levels of Cathepsin B/D, cleaved-caspase-3, Bax, Ferritin and TfR. In addition, DFO and LAP treatments attenuated intimal injury by alleviating HUVECs apoptosis and degradation. In experiment 3, we also found that DFO and LAP treatments both inhibited the apoptosis pathway mediated by intralysosomal Cathepsins by reducing the levels of Cathepsin B/D, cleaved-caspase-3, Bax, Ferritin and TfR. In addition, DFO and LAP treatments attenuated HUVECs injury by alleviating HUVECs apoptosis and degradation, reducing mitochondrial damage and maintaining lysosomal integrity after OxyHb stimulating.

Currently, vascular endothelium damage caused by iron overload in assosiation with oxidative stress and the partial underlying mechanisms has not been confirmed yet. The prolonged exposure to iron increases endothelial NADPH oxidase activity by increasing p22phox gene transcription and cellular levels of iron, heme, and p22phox protein. DFO effectually suppresses endothelial NADPH oxidase activity, which may be helpful as an drug in reducing vascular oxidative stress and inflammation in atherosclerosis [28]. Excessive ROS activated ROS-induced ROS release (RIRR) mechanism, reduced mitochondrial membrane potential (MMP), and opened mitochondrial permeability transition pore (mPTP), thereby led to mitochondrial function dysfunction [11]. In addition, iron could induce endothelial microparticles generation and apoptosis of ECs related to increased oxidative stress and carvedilol could provide the protection via inhibiting these mechanisms [13]. The recent research findings also revealed that Nobiletin could protect HUVECs against iron overloaded damage, and the mechanism may be associated with restraining the ROS/ADMA/DDAHII/eNOS/NO pathway. Specifically speaking, Nobiletin could reduce oxidative stress and ROS generation, increase DDAHII expression and activity and NO production, promote eNOS phosphorylation, decrease ADMA content to maintain mitochondrial function, and protect vascular endothelium against iron overload induced damage [29]. In transient forebrain ischemia rat models, iron overload and iron-mediated free radical production aggravate BBB injury via decreasing tight junction proteins expressions and increasing degeneration of ECs [12]. In addition, iron overload induces

ured vascular cells apoptosis, which aggravates

atherosclerosis progression, simultaneously, Iron intake restriction or iron chelation therapy can suppress iron-aggravated atherosclerosis in ApoE-/- FPNwt/C326S mice model [30]. In our experiment, we found that Iron could increase oxidative stress level and increase lysosomal membrane permeability. Thus, the leaked Cathepsins from ruptured lysosomes activated mitochondrial apoptotic pathway and damaged HUVECs. The additional important results were obtained that the content of ROS and MDA and activities of SOD and GSH-Px were inhibited by LAP in endothelium and HUVECs suggested that LAP seemingly had a more potent capacity of resisting oxidative stress by scavenging ROS and lowering ROS generation in the lysosomes and cytoplasm via interacting with lysosomal iron compared to DFO.

Endothelial dysfunction was closely associated with IH formation and several drugs were discovered to inhibit endothelial dysfunction. The previous study found that Anagliptin, the dipeptidyl peptidase IV (DPP-4) inhibitor suppresses IH via preventing endothelial dysfunction and regulating SOD-1/RhoA/JNK-mediated ECs migration after balloon injury [31]. Moreover, the novel mineralocorticoid receptor antagonist, finerenone significantly reduces apoptosis of ECs and simultaneously attenuates SMC proliferation, resulting in accelerated endothelial healing and reduced neointima formation of the injured vessels. Thus, finerenone appears to provide favorable vascular effects through restoring vascular integrity and preventing adverse vascular remodeling [32]. Besides, low dosage of simvastatin can induce cardiac microvascular ECs proliferation, migration and anti-apoptosis via PI3K/Akt/mTOR/p70S6K and mTOR/FoxO3 signalling pathways, and then exert a beneficial effect by regulation of NO and ROS production in microvascular ECs [33]. In our research, we also confirmed that iron evidently aggravated ECs injury via aggravating lysosomal injury and LAP could alleviate ECs injury triggered by redox-active iron decomposed by OxyHb. Therefore, LAP had a more powerful capacity to chelating iron than DFO due to its high concentration and reduced form. Overall, we drew a conclusion that not only LAP was a more potent antioxidant but also was a kind of agent of lysosomal membrane stabilizing and iron chelating which targeted lysosomes in accordance with the results from our study.

Hence, we proposed this research hypotheses that partial erythrocytes attached to the walls of the blood vessels and were decomposed into iron after CA intima damage, which was transferred into the ECs cytoplasm through combination of TfRs. A lot of unstable and intralysosomal iron formation by lysosomal endocytosis and degradation and accelerated more hydroxyl radical generation via Fenton reaction. Abundant hydroxyl radical disrupted lysosomal membrane and increased the lysosomal membrane permeability. Next, a variety of Cathepsins released into the cytoplasm and activated the apoptosis pathway mediated by mitochondria, which accelerated ECs apoptosis and delayed endothelial repair in injured region. LAP, as a kind of lysosomotropic and iron-chelating agent, could target to gathering in lysosomes and inhibit the reaction of Fenton reaction by reacting with active iron. Hence, LAP inhibited the apoptosis pathway mediated by mitochondria by reducing the generation of hydroxyl radicals, stabilizing the lysosome membrane and decreasing the release of cathepsins. Ultimately, LAP reduced the ECs apoptosis and injury, promoted the re-endothelialization of the damaged area, inhibited the excessive proliferation of vascular intima and reduced the rate of vascular restenosis. A possible mechanism that that LAP reduced the intimal injury was shown in Fig. 11.

The current study has some limitations. Firstly, the precise concentration of intralysosomal iron in ECs could not be measured precisely relying on our current experimental platform. Secondly, we could not detect the distribution of reduced LAP within lysosomes in ECs. In summary, this study suggested that LAP exerted a stronger endovascular protection than DFO, and the underlying mechanisms may be that LAP inhibited signaling pathways mediated by Cathepsins via interacting with intralysosomal iron. Consequently, some drugs could have great therapeutic prospects for treating endovascular injury, such as LAP, which could target lysosomes and chelate iron.

Declarations

Author contributions: Study conception and design, quality assurance and control: XPW, CSN; experimental implementation and manuscript writing: YW, XQK; analytic strategy design: DJB; literature review, materials preparation and methods section: BX; manuscript reviewing and editing: YFD. All authors approved the final version of the paper.

Compliance with Ethical Standards

Conflict of Interest The authors declare that they have no conflict of interest.

Ethical Approval All applicable international, national, and/or institutional guidelines for the care and use of animals were followed.

Funding: This study was supported by the National Natural Science Foundation of China, No. 81500375 (to XQK), the Fundamental Research Funds for the Central Universities, No. WK9110000112 (to YW), the Anhui Provincial Natural Science Foundation of China, No. 1508085QH184 (to YW), and Shandong Provincial Natural Science Foundation of China, No. ZR2015HQ001 (to XQK).

References

1. Brinjikji W, Huston J, Rabinstein AA, Kim GM, Lerman A, Lanzino G. Contemporary carotid imaging: from degree of stenosis to plaque vulnerability. J Neurosurg. 2016;124:27-42.
2. Dharmakidari S, Bhattacharya P, Chaturvedi S. Carotid Artery Stenosis: Medical Therapy, Surgery, and Stenting. Curr Neurol Neurosci Rep. 2017;17:77.
3. Röhl S, Eriksson L, Saxelin R, et al. Noninvasive in vivo Assessment of the Re-endothelialization Process Using Ultrasound Biomicroscopy in the Rat Carotid Artery Balloon Injury Model. J Ultrasound Med. 2019;38:1723-1731.
4. Allagnat F, Dubuis C, Lambelet M, et al. Connexin37 reduces smooth muscle cell proliferation and intimal hyperplasia in a mouse model of carotid artery ligation. Cardiovasc Res. 2017;113:805-816.
5. Goldstone RN, McCormack MC, Goldstein RL, et al. Photochemical Tissue Passivation Attenuates AV Fistula Intimal Hyperplasia. Ann Surg. 2018;267:183-188.

6. Icli B, Wu W, Ozdemir D, et al. MicroRNA-135a-3p regulates angiogenesis and tissue repair by targeting p38 signaling in endothelial cells. FASEB J. 2019;33:5599-5614.
7. Michel JB, Martin-Ventura JL. Red Blood Cells and Hemoglobin in Human Atherosclerosis and Related Arterial Diseases. Int J Mol Sci. 2020;21:6756.
8. Zhang J, Cai W, Fan Z, et al. MicroRNA-24 inhibits the oxidative stress induced by vascular injury by activating the Nrf2/Ho-1 signaling pathway. Atherosclerosis. 2019;290:9-18.
9. DeGregorio-Rocasolano N, Martí-Sistac O, Gasull T. Deciphering the Iron Side of Stroke: Neurodegeneration at the Crossroads Between Iron Dyshomeostasis, Excitotoxicity, and Ferroptosis. Front Neurosci. 2019;13:85.
10. Chan S, Lian Q, Chen MP, et al. Deferiprone inhibits iron overload-induced tissue factor bearing endothelial microparticle generation by inhibition oxidative stress induced mitochondrial injury, and apoptosis. Toxicol Appl Pharmacol. 2018;338:148-158.
11. He H, Qiao Y, Zhou Q, et al. Iron Overload Damages the Endothelial Mitochondria *via*the ROS/ADMA/DDAHII/eNOS/NO Pathway. Oxid Med Cell Longev. 2019:2340392.
12. Won SM, Lee JH, Park UJ, Gwag J, Gwag BJ, Lee YB. Iron mediates endothelial cell damage and blood-brain barrier opening in the hippocampus after transient forebrain ischemia in rats. Exp Mol Med. 2011;43:121-8.
13. Chan S, Chen MP, Cao JM, Chan GC, Cheung YF. Carvedilol protects against iron-induced microparticle generation and apoptosis of endothelial cells. Acta Haematol. 2014;132:200-10.
14. Persson HL, Yu Z, Tirosh O, Eaton JW, Brunk UT. Prevention of oxidant-induced cell death by lysosomotropic iron chelators. Free Radic Biol Med. 2003;34:1295-305.
15. Wang Y, Gao A, Xu X, et al. The Neuroprotection of Lysosomotropic Agents in Experimental Subarachnoid Hemorrhage Probably Involving the Apoptosis Pathway Triggering by Cathepsins via Chelating Intralysosomal Iron. Mol Neurobiol. 2015;52:64-77.
16. Yu ZQ, Jia Y, Chen G. Possible involvement of cathepsin B/D and caspase-3 in deferoxamine-related neuroprotection of early brain injury after subarachnoid haemorrhage in rats. Neuropathol Appl Neurobiol. 2014;40:270-83.
17. Chen D, Tao X, Wang Y, Tian F, et al. Curcumin accelerates reendothelialization and ameliorates intimal hyperplasia in balloon-injured rat carotid artery via the upregulation of endothelial cell autophagy. Int J Mol Med. 2015;36:1563-71.
18. Lee YC, Chang YC, Wu CC, Huang CC. Hypoxia-Preconditioned Human Umbilical Vein Endothelial Cells Protect Against Neurovascular Damage After Hypoxic Ischemia in Neonatal Brain. Mol Neurobiol. 2018;55:7743-7757.
19. Yuan S, Yu Z, Zhang Z, Zhang J, et al. RIP3 participates in early brain injury after experimental subarachnoid hemorrhage in rats by inducing necroptosis. Neurobiol Dis. 2019;129:144-158.
20. Shen F, Xu X, Yu Z, et al. Rbfox-1 contributes to CaMKIIα expression and intracerebral hemorrhage-induced secondary brain injury via blocking micro-RNA-124. J Cereb Blood Flow Metab. 2020;

21. Zhou S, Yin T, Zou Q, et al. Labeling adipose derived stem cell sheet by ultrasmall superparamagnetic Fe3O4 nanoparticles and magnetic resonance tracking in vivo. Sci Rep. 2017;7:42793.
22. Wang Y, Bao DJ, Xu B, et al. Neuroprotection mediated by the Wnt/Frizzled signaling pathway in early brain injury induced by subarachnoid hemorrhage. Neural Regen Res. 2019;14:1013-1024.
23. Chen X, Jiang M, Li H, et al. CX3CL1/CX3CR1 axis attenuates early brain injury via promoting the delivery of exosomal microRNA-124 from neuron to microglia after subarachnoid hemorrhage. J Neuroinflammation. 2020;17:209.
24. Lv TZ, Wang GS. Antiproliferation potential of withaferin A on human osteosarcoma cells via the inhibition of G2/M checkpoint proteins. Exp Ther Med. 2015;10:323-329.
25. Yang SD, Yang DL, Sun YP, et al. 17β-estradiol protects against apoptosis induced by interleukin-1β in rat nucleus pulposus cells by down-regulating MMP-3 and MMP-13. Apoptosis. 2015;20:348-57.
26. Li B, Zhang Y, Li H, et al. Miro1 Regulates Neuronal Mitochondrial Transport and Distribution to Alleviate Neuronal Damage in Secondary Brain Injury After Intracerebral Hemorrhage in Rats. Cell Mol Neurobiol. 2020 Jun 4.
27. Han J, Huang C, Jiang J, Jiang D. Activation of autophagy during farnesyl pyrophosphate synthase inhibition is mediated through PI3K/AKT/mTOR signaling. J Int Med Res. 2020;48:300060519875371.
28. Li L, Frei B. Prolonged exposure to LPS increases iron, heme, and p22phox levels and NADPH oxidase activity in human aortic endothelial cells: inhibition by desferrioxamine. Arterioscler Thromb Vasc Biol. 2009;29:732-8.
29. Wang Z, Yang B, Chen X, et al. Nobiletin Regulates ROS/ADMA/DDAHII/eNOS/NO Pathway and Alleviates Vascular Endothelium Injury by Iron Overload. Biol Trace Elem Res. 2020;198:87-97.
30. Vinchi F, Porto G, Simmelbauer A, et al. Atherosclerosis is aggravated by iron overload and ameliorated by dietary and pharmacological iron restriction. Eur Heart J. 2020;41:2681-2695.
31. Li Q, Zhang M, Xuan L, Liu Y, Chen C. Anagliptin inhibits neointimal hyperplasia after balloon injury via endothelial cell-specific modulation of SOD-1/RhoA/JNK signaling in the arterial wall. Free Radic Biol Med. 2018;121:105-116.
32. Dutzmann J, Musmann RJ, Haertlé M, et al. The novel mineralocorticoid receptor antagonist finerenone attenuates neointima formation after vascular injury. PLoS One. 2017;12:e0184888.
33. Pan Q, Xie X, Guo Y, Wang H. Simvastatin promotes cardiac microvascular endothelial cells proliferation, migration and survival by phosphorylation of p70 S6K and FoxO3a. Cell Biol Int. 2014;38:599-609.

Figures

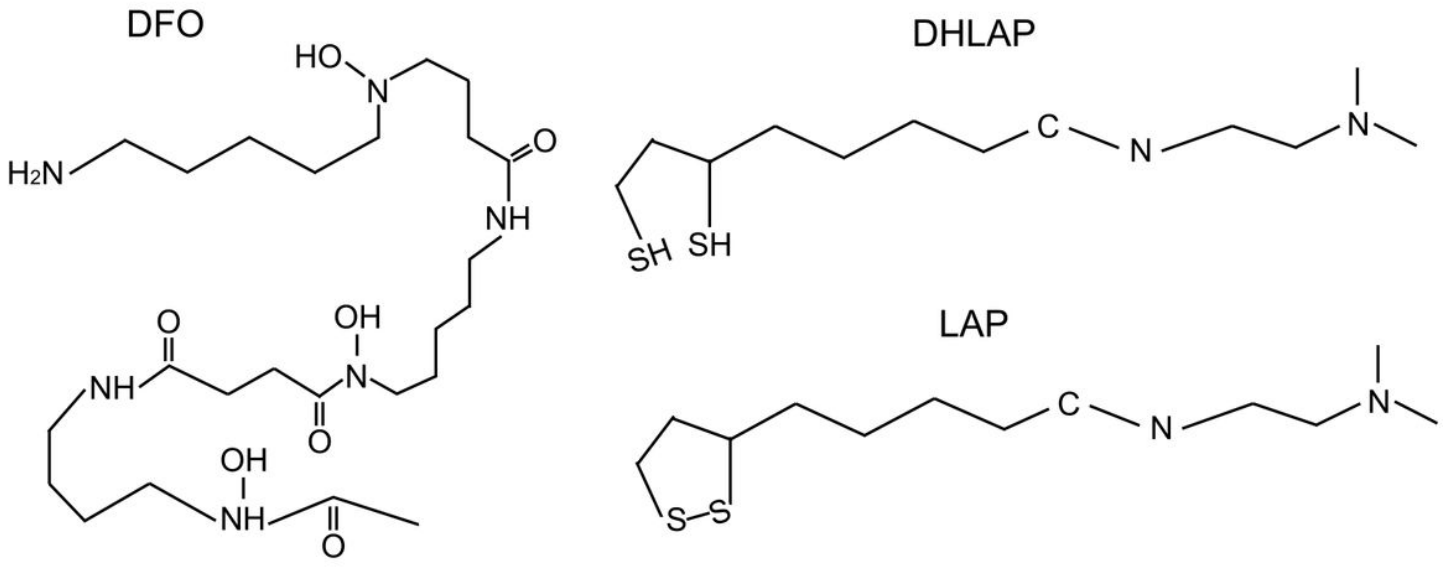

Figure 1

Structures of DFO, LAP, and DHLAP

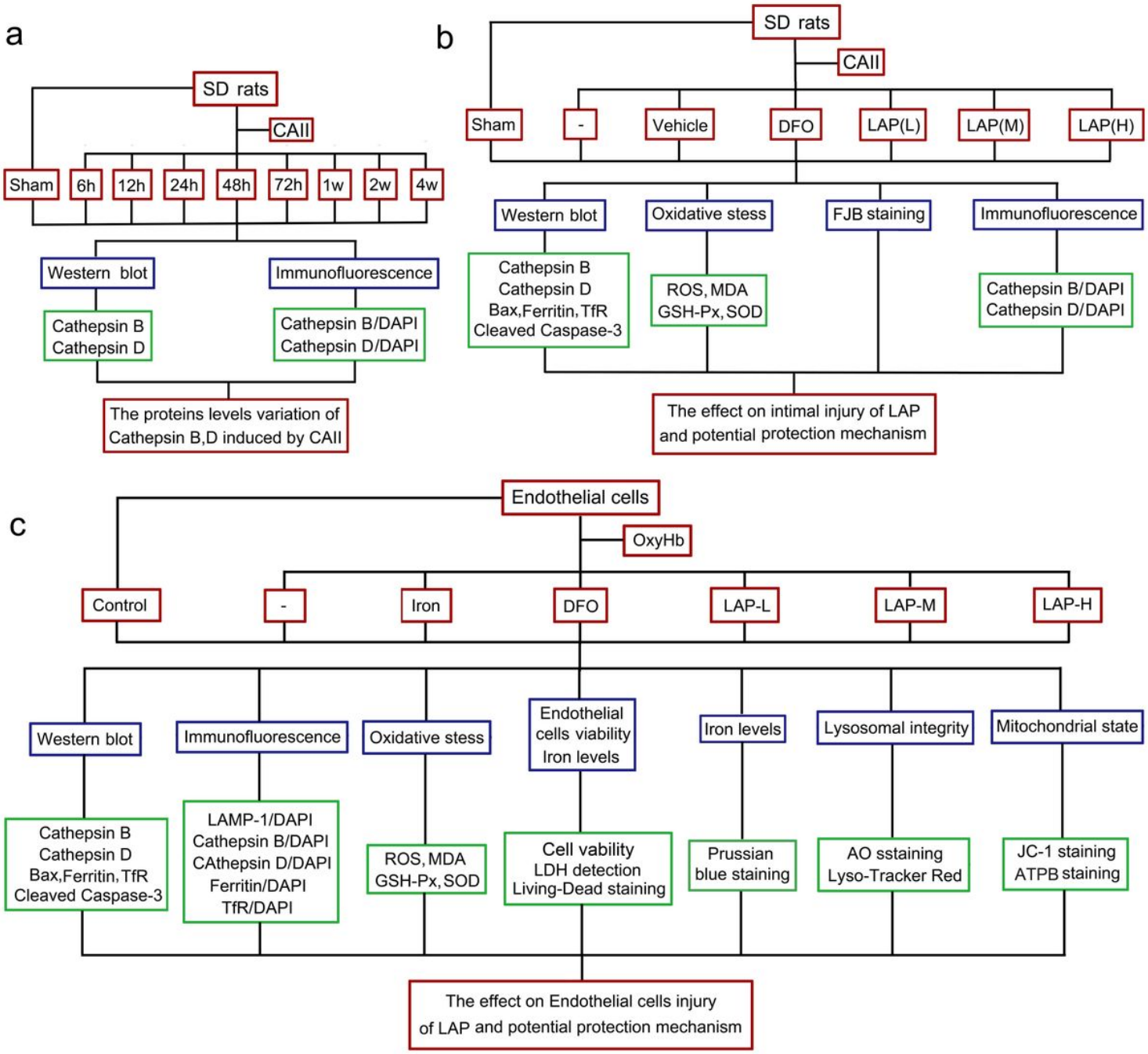

Figure 2

Experimental design. (a) Experiments 1was designed to determine involvement of Cathepsin B/D under CAII condition. (b) Experiment 2 was designed for exploring the mechanisms of LAP alleviating endothelial injury induced by CAII. (c) Experiment 3 was designed for exploring the roles and mechanisms of LAP alleviating HUVECs injury induced by OxyHb in vitro.

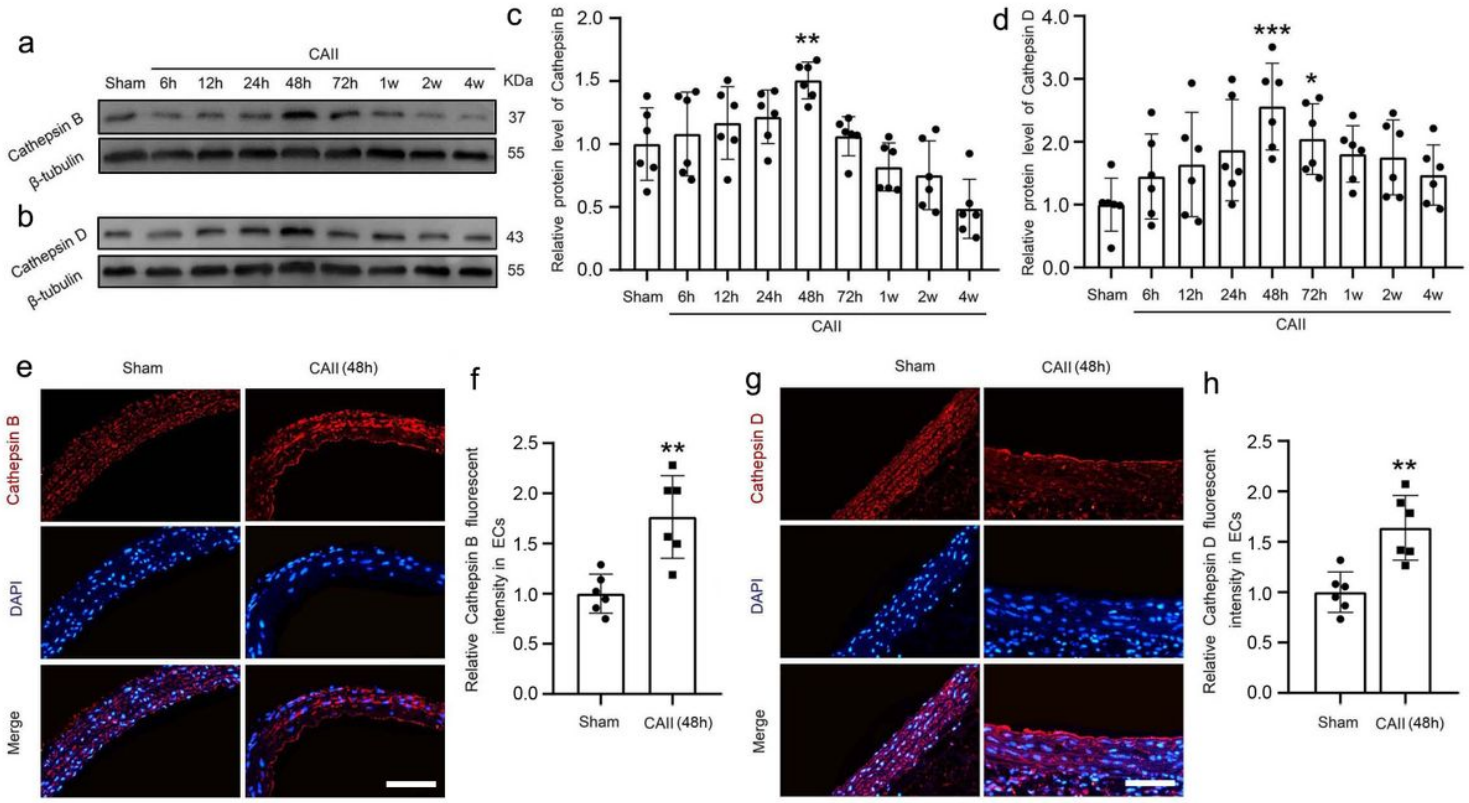

Figure 3

Time course of the protein levels of Cathepsin B/D after CAII. (a, b) Western blotting showing the protein levels of Cathepsin B/D at Sham, 6, 12, 24, 48, 72 h, 1w, 2w as well as at 4w after CAII. (c, d) Quantification of Cathepsin B/D protein levels were normalized to that of β-tubulin. (e, g) Immunofluorescent analysis was performed with antibodies for Cathepsin B/D (red) in CAII sections. Nuclei were labeled with DAPI (blue). Representative images of the Sham group and CAII (48 h) group are shown. Scale bar = 100 μm. (f, h) Immunopositivities of Cathepsin B/D in the endothelium. The Sham group was used as the standard. Data were shown as the mean ± SEM (n = 6). *P < 0.05, **P < 0.01, ***P < 0.001 vs. Sham group.

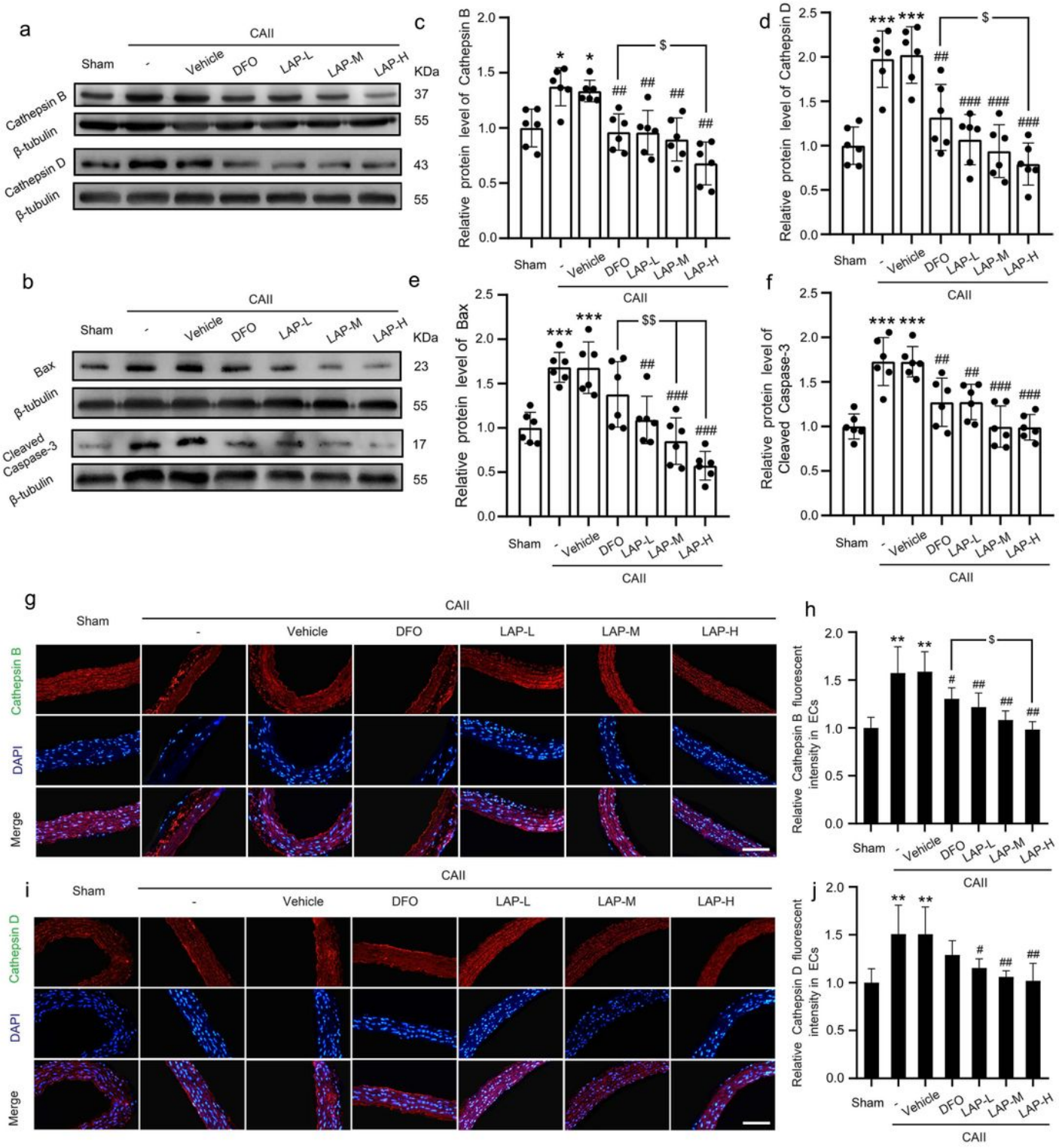

Figure 4

Changes in Cathepsin B/D, cleaved-caspase-3, Bax after DFO and LAP treatments under CAII conditions. (a, b) Western blot analysis showed that Cathepsin B/D, cleaved-caspase-3, Bax expressions in Sham group, CAII, CAII + Vehicle group, CAII + DFO group, CAII + LAP (L) group, CAII + LAP (M) group and CAII + LAP (H) group. (c-f) The mean values of the protein levels Cathepsin B/D, cleaved-caspase-3, Bax in

mmunofluorescence analysis was performed with Cathepsin

B/D antibodies (green), and nuclei were fluorescently labeled with DAPI (blue). (h, j) The mean value of the fluorescent intensity of Sham group was normalized to 1.0. Scale bar= 100 μm. Data are means ± SEM. *P < 0.05, **P < 0.01, ***P < 0.001 vs. Sham group; #P<0.05, ##P<0.01, ###P<0.001 vs. CAII + Vehicle group; $P<0.05, $$P<0.01 vs. CAII + DFO group, n=6.

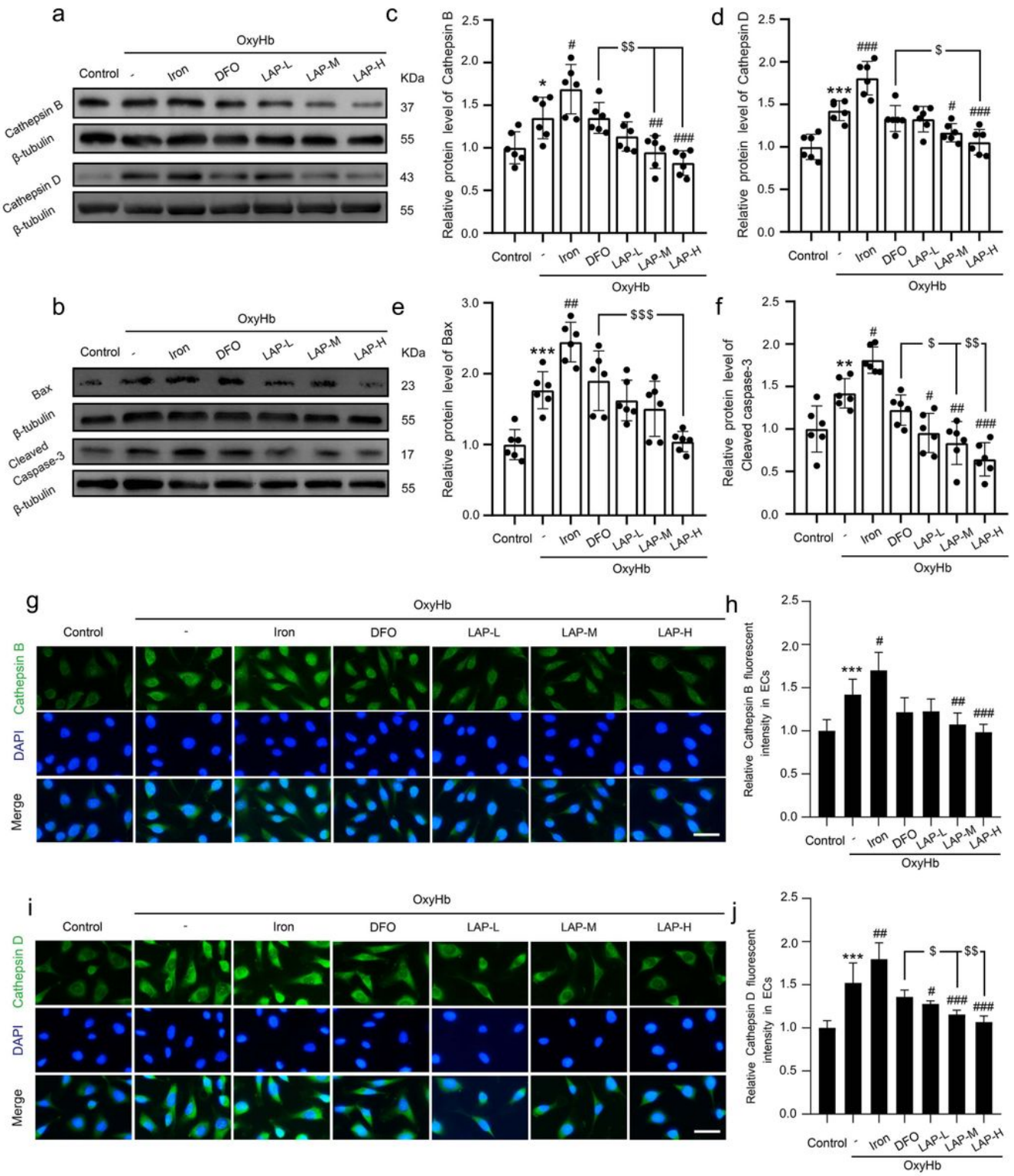

Figure 5

Changes in Cathepsin B/D, cleaved-caspase-3, Bax after DFO and LAP treatments under HUVECs injury conditions. (a, b) Western blot analysis showed that Cathepsin B/D, cleaved-caspase-3, Bax expressions in Control group, OxyHb, OxyHb + Iron group, OxyHb + DFO group, OxyHb + LAP (L) group, OxyHb + LAP (M) group and OxyHb + LAP (H) group. (c-f) The mean values of the protein levels Cathepsin B/D, cleaved-caspase-3, Bax in Control group were normalized to 1.0. (g, i) Immunofluorescence analysis was performed with Cathepsin B/D antibodies (green), and nuclei were fluorescently labeled with DAPI (blue). (h, j) The mean value of the fluorescent intensity of Control group was normalized to 1.0. Scale bar= 100 μm. Data are means ± SEM. *P<0.05, **P<0.01, ***P<0.001 vs. Control group; #P<0.05, ##P<0.01, ###P<0.001 vs. OxyHb group; $P<0.05,

$$P < 0.01,$$

$P<0.001 vs. OxyHb + DFO group, n=6.

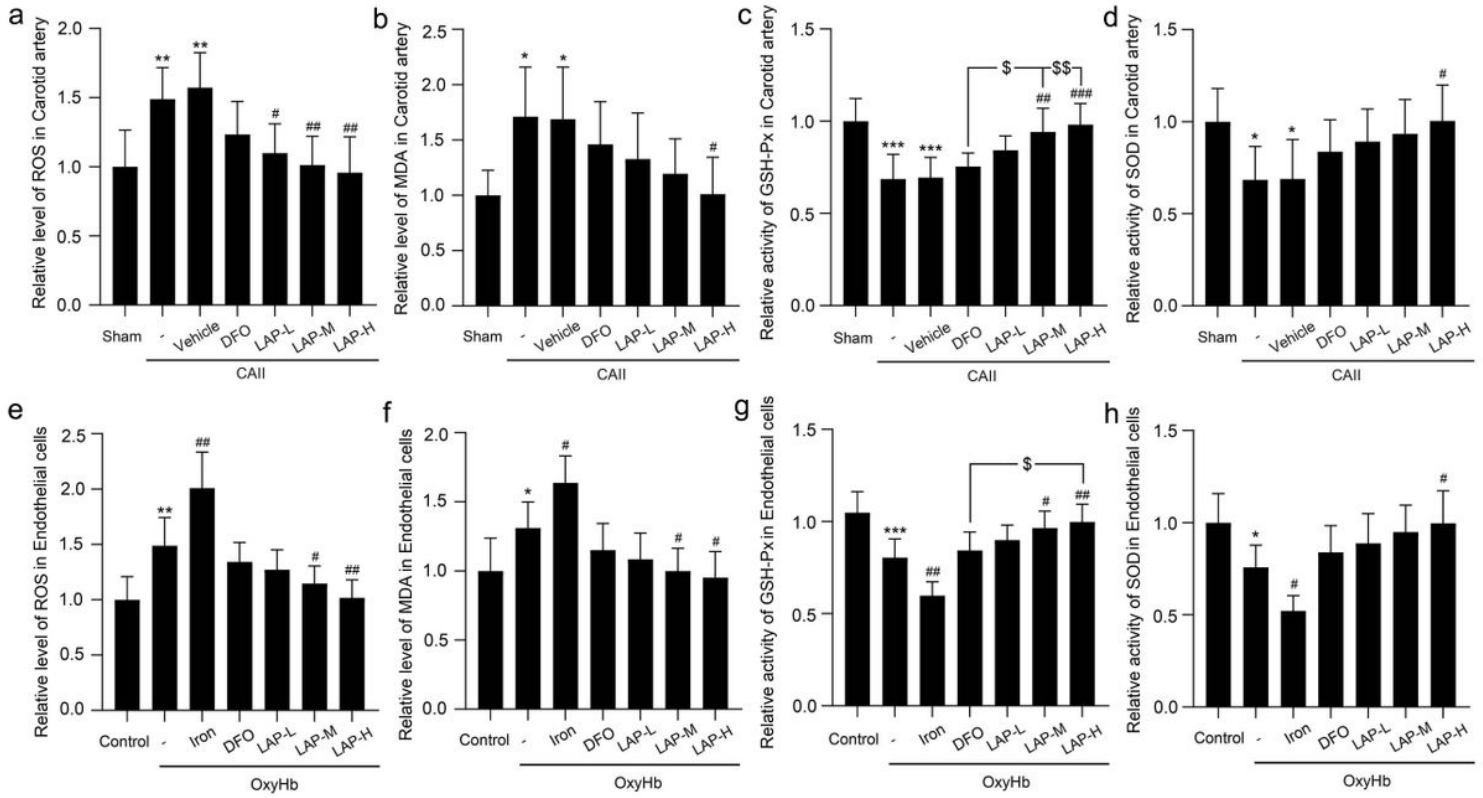

Figure 6

The variation of oxidative stress after DFO and LAP administration under endothelium and HUVECs injury conditions. The measurement of oxidative stress after DFO and LAP administrations in endothelium tissue (a-d) and HUVECs (e-h). The mean values of the levels of ROS, MDA, and the activities of SOD and GSH-Px of Sham and Control group was normalized to 1.0. Data are means ± SEM. *P<0.05, **P<0.01, ***P<0.001 vs. Sham and Control group; #P<0.05, ##P<0.01, ###P<0.01 vs. CAII + Vehicle and OxyHb group; $P<0.05, $$P<0.01 vs. CAII + DFO group and OxyHb + DFO group, n=6.

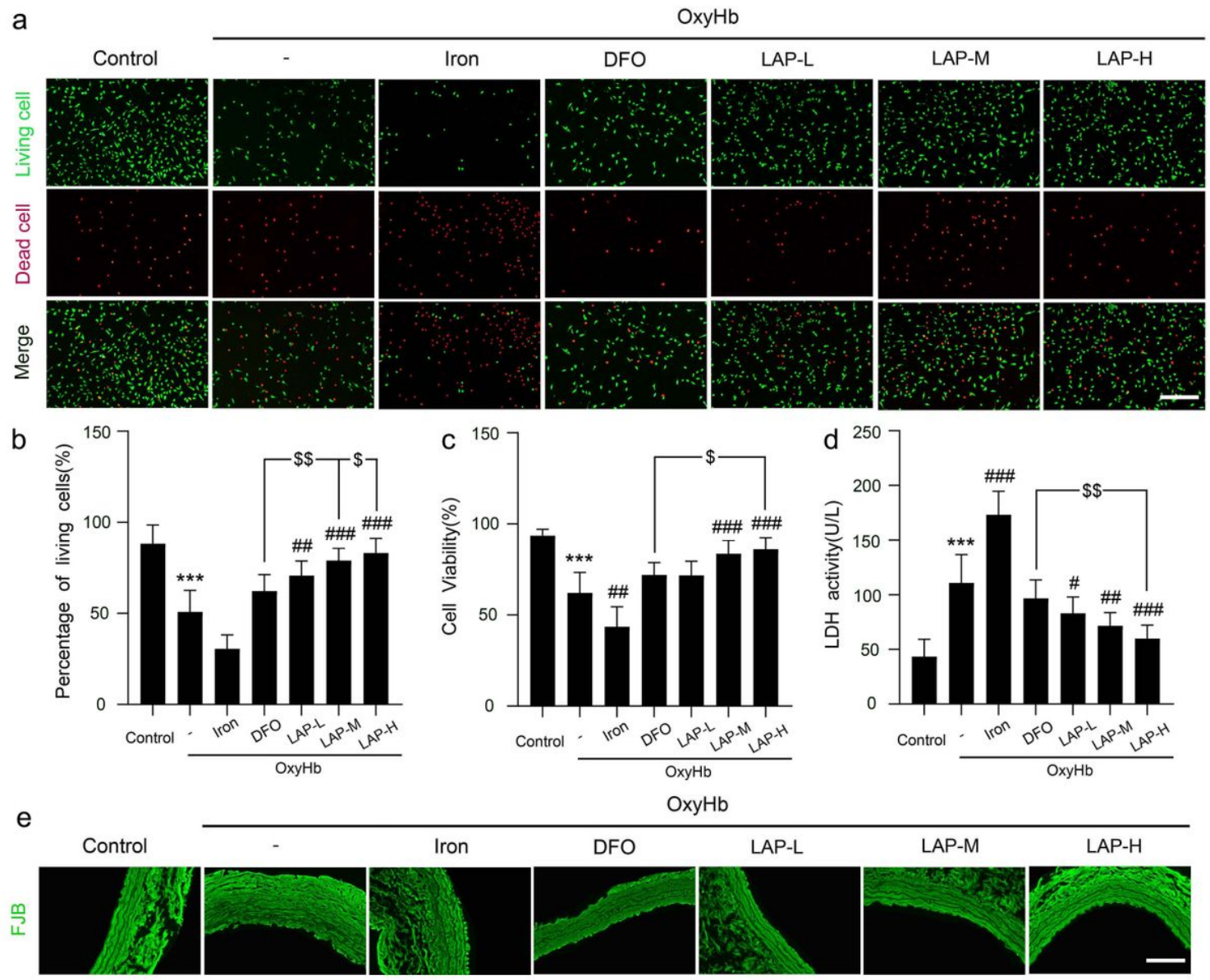

Figure 7

Effect of mitochondria damage after DFO and different dosages LAP treatments under HUVECs injury conditions (a) Immunofluorescence analysis was performed with ATPB antibodies for (green), and nuclei were fluorescently labeled with DAPI (blue). (b) Alterations in mitochondrial membrane potential (ΔΨm). The presence of red fluorescence indicates normal ΔΨm and a healthy state of the cells. Green fluorescence indicates that the ΔΨm had decreased, and that the cells were most likely to be in the early stage of apoptosis. (c) The mean value of the fluorescent intensity of Control group was normalized to 1.0. (d) JC-1 immunofluorescence intensity ratio (Red/Green) in HUVECs in Control group, OxyHb, OxyHb + Iron group, OxyHb + DFO group, OxyHb + LAP (L) group, OxyHb + LAP (M) group and OxyHb + LAP (H) group. Scale bar= 100 μm. Data are means ± SEM. ***P<0.001 vs. Control group; #P<0.05, ###P<0.001 vs. OxyHb group; $P<0.05,

$$P < 0.01,$$

$P<0.001 vs. OxyHb + DFO group, n=6.

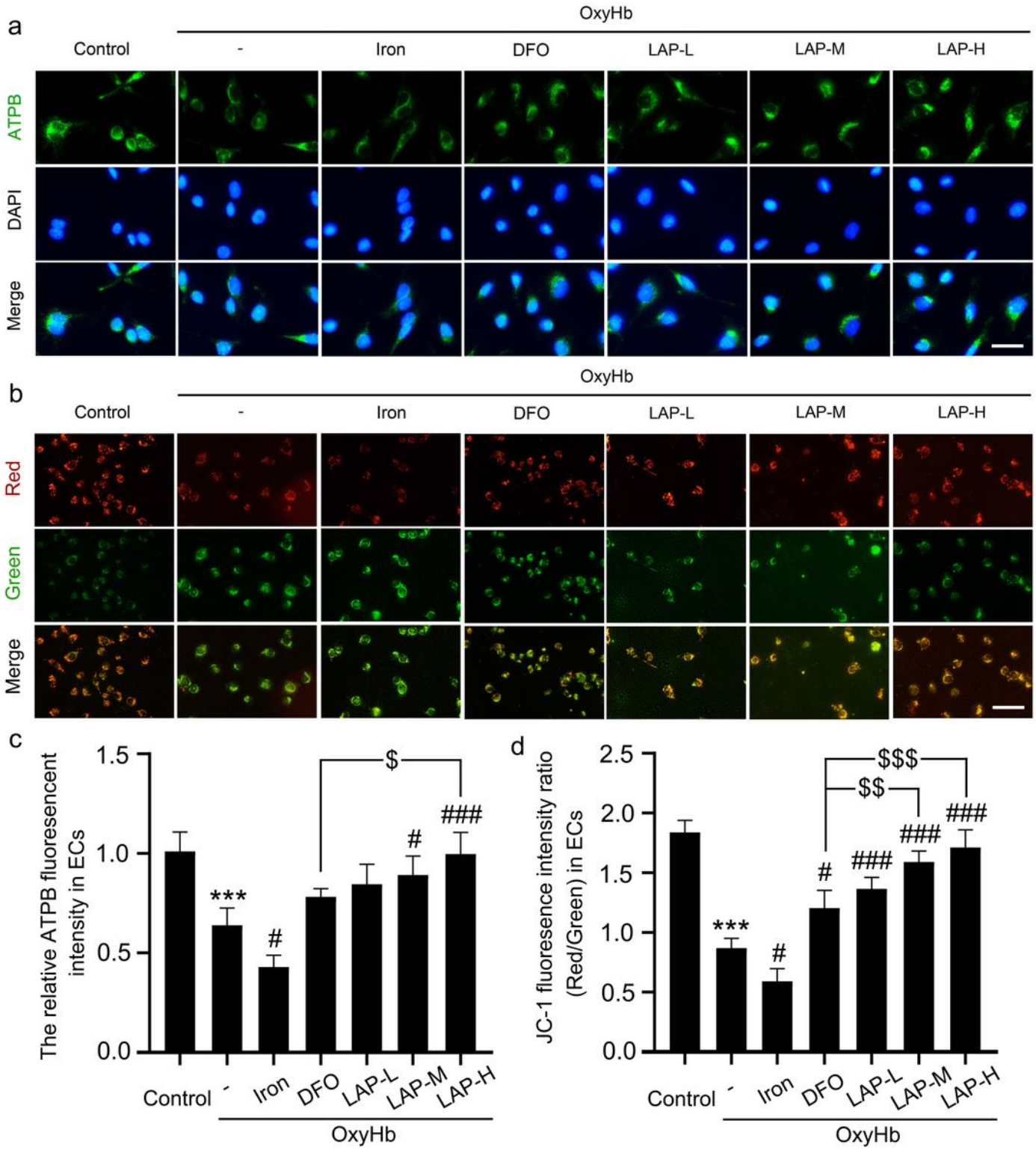

Figure 8

LAP attenuates cellular damage and improves cellular viability in vitro. (a) Live-dead cellular staining: green staining indicates viable cells and red staining indicates dead cells. (b) The percentage of living cells revealed by live-dead cellular staining. (c) Cell viability was tested by the SRB assay in HUVECs. (d)

tured HUVECs. (e) The neuronal degeneration at 48 hours

after CAII was detected by FJB staining (green). Arrows pointed to FJB-positive cells. Scale bar =100 μm. Data are means ± SEM. ***P<0.001 vs. Control group; #P<0.05, ##P<0.01, ###P<0.001 vs. OxyHb group; $P<0.05, $$P<0.01 vs. OxyHb + DFO group, n=6.

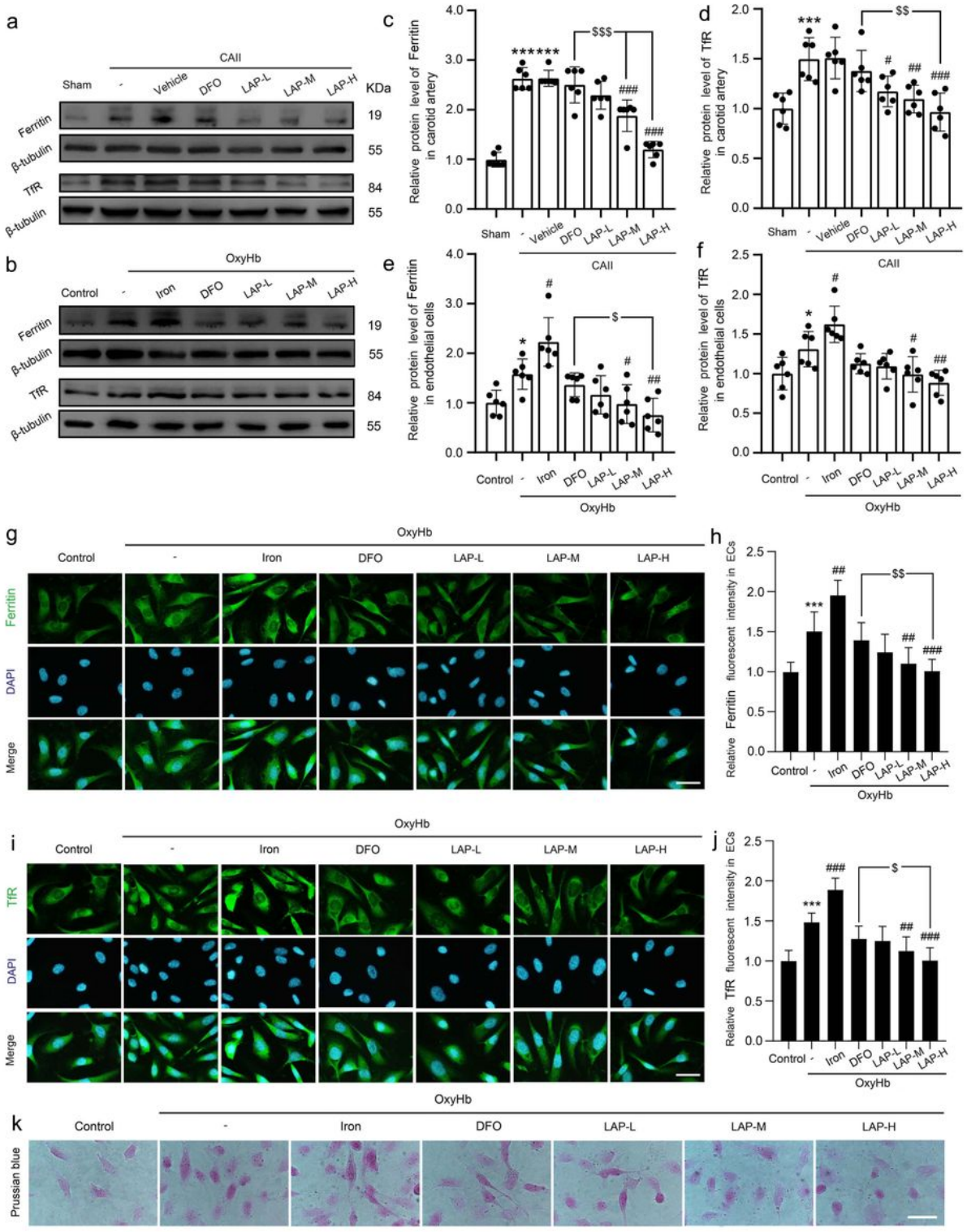

Figure 9

Changes in Ferritin and TfR after DFO and LAP treatments under endothelium and HUVECs injury

d that Ferritin and TfR expressions in Sham group, CAII, CAII +

vehicle group, CAII + DFO group, CAII + LAP (L) group, CAII + LAP (M) group and CAII + LAP (H) group. (b) Western blot analysis showed that Ferritin and TfR expressions in Control group, OxyHb, OxyHb + Iron group, OxyHb + DFO group, OxyHb + LAP (L) group, OxyHb + LAP (M) group and OxyHb + LAP (H) group. (c-f) The mean values of the protein levels Ferritin and TfR in Sham group and Control group were normalized to 1.0. (g, i) Immunofluorescence analysis was performed with Ferritin and TfR antibodies (green), and nuclei were fluorescently labeled with DAPI (blue). (h, j) The mean value of the fluorescent intensity of Control group was normalized to 1.0. (k) Iron deposition or iron clusters in the HUVECs were observed in different groups. Representative images were shown. Scale bar= 100 μm. Data are means ± SEM. *P<0.05, ***P<0.001 vs. Sham group and Control group; #P<0.05, ##P<0.01, ###P<0.001 vs. CAII + Vehicle group and OxyHb group; $P<0.05,

$$P < 0.01,$$

$P<0.001 vs. CAII + DFO group and OxyHb + DFO group, n=6.

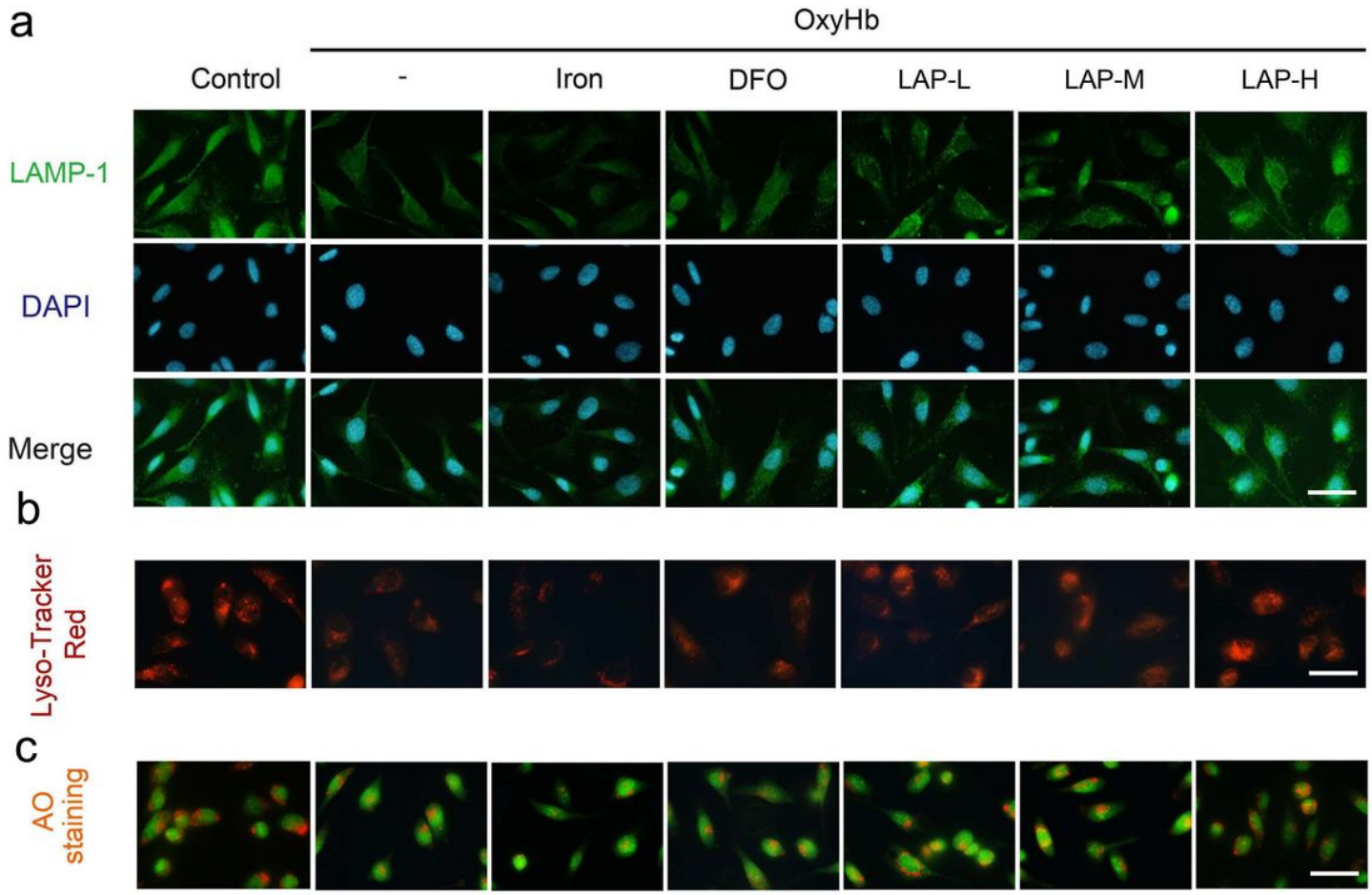

Figure 10

Effect of lysosomal integrity after DFO and different dosages LAP treatments under HUVECs injury conditions. (a) Immunofluorescence analysis was performed with LAMP-1 antibodies for (green), and nuclei were fluorescently labeled with DAPI (blue). (b) Lyso-Traker Red cellular staining: red staining

indicates intact lysosomes in HUVECs. (c) AO staining: orange staining indicates acidic compartment accumulation in HUVECs.

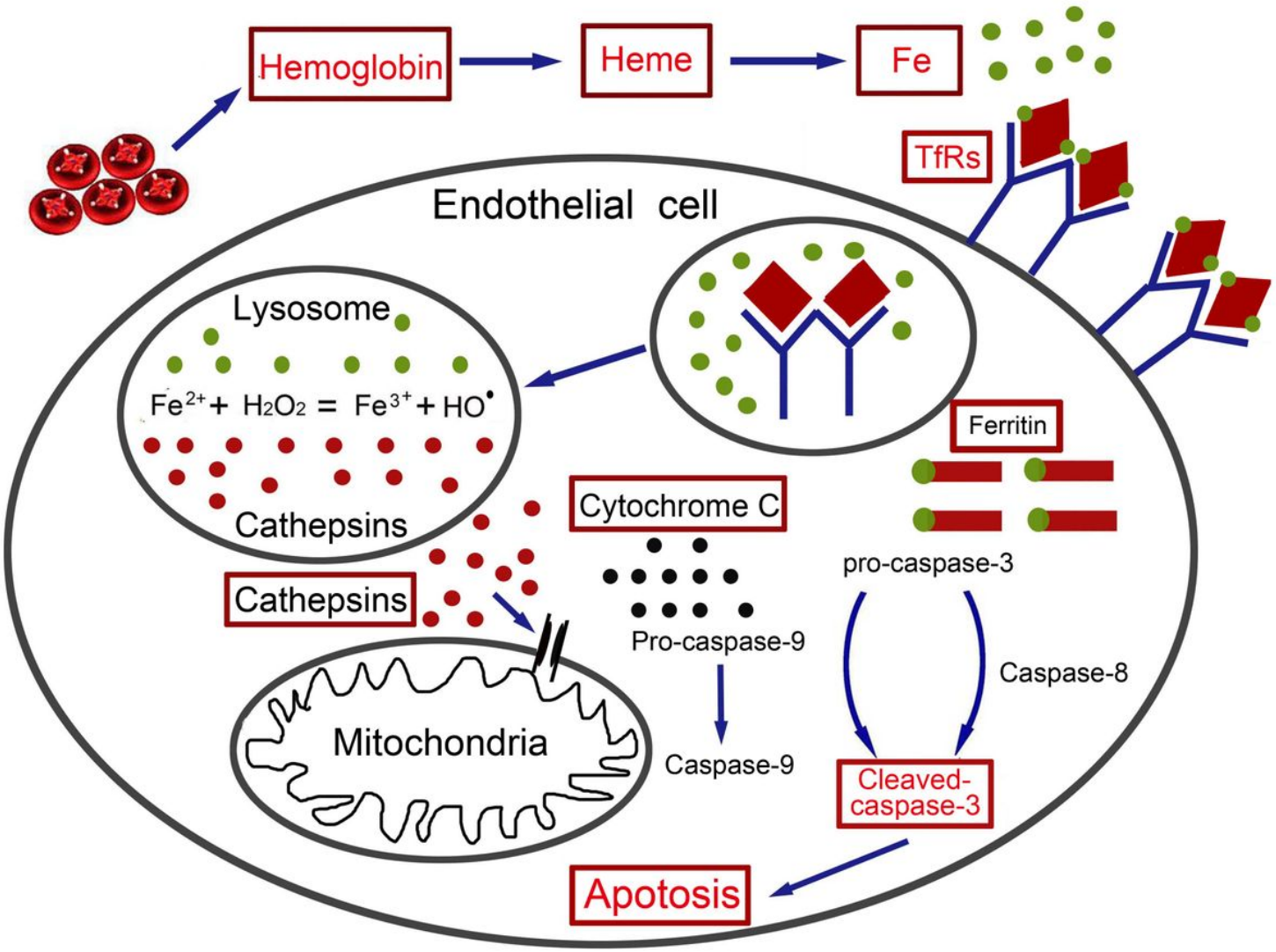

Figure 11

Potential mechanisms suggesting that LAP alleviates HUVECs and endothelium damage via inhibiting mitochondrial apoptosis pathway triggered by lysosomal Cathepsins.